Adapted nonlinear multiresolution decomposition with applications in progressive lossless image coding

Michel Barret and hocine Bekkouche[*]

Supélec

Équipe Signaux et Systèmes Électroniques

2 rue É. Belin 57070 Metz (France)

Michel.Barret@supelec.fr, Hocine.Bekkouche@supelec.fr

June 18, 2002

Abstract

We present an adapted nonlinear multiresolution decomposition (with some derivatives) of still images that permits perfect reconstruction. A hierarchical pyramidal decomposition with maximal decimation is used. For one level of decomposition, the input image I is partitioned into two subimages I_1 and I_2 obtained by down-sampling. The subimage I_1 is unchanged. The subimage I_2 is replaced by the rounded output I_h of a 2D FIR filter whose coefficients have first been adapted to I and which has the entries I_1 and I_2. A similar processing is then applied one time to each of the subimages I_1 and I_h. The nonlinearity introduced by the rounding permits to perfectly inverse the process, even when inverse filters (which are all ARMA) are not BIBO stable. Applications are given in lossless image coding, with possibility of embedded zerotree coding.

1 Introduction

Lossless image compression with embedded coding is well suited to image transmission, where the user wants to display a low quality image quickly and then successively improves it until lossless transmission, if wished. This kind of image transmission finds applications in various domains, like archiving, medical or satellite image processing. The advantage of the embedded coding is to give the user a total control of the precision in which the image pixels are represented. These image coding techniques, like the embedded zerotree wavelet (EZW) algorithm introduced by Shapiro [11] and the SPIHT algorithm introduced by Said and Pearlman [10] are based on a multiresolution decomposition—with unitary transforms—of the input image. These algorithms are today widely used in various applications, particularly for lossy or nearly lossless image compression.

Over the last years, papers presenting performances of lossless image codecs based on multiresolution decompositions have been published. Some of them use wavelet decompositions [1, 7] and some others use subband decompositions with adaptive or nonlinear filters [5, 6]. In [5], the authors use a polyphase subband decomposition, associated with a LMS adaptation, where the estimation filter coefficients are updated according to a gradient type algorithm.

In this paper we study a special frame of the nonlinear subband decomposition with perfect reconstruction given in [6]. A major difference with our approach is that the decomposition and reconstruction filterbanks are adapted to the input image, in order to minimize a mean square error. More-

over, the adaptive polyphase subband decomposition structures used in [5] for image compression differ from ours in three points: the first one is that we use nonlinear filterbanks (this possibility is already mentioned in [5] but is not used), the second one is that we do not update the filters coefficients pixel per pixel (the method we use in order to adapt the filters coefficients to the input image is global) and the third one is that we use ARMA filters (and not just 2D FIR filters). This allows to appreciably reduce the mean square error. The second point is also very important for applications in lossless image coding. Our method allows embedded zerotree coding whereas an adaptive method could not, because it would be impossible to properly update the filters coefficients at the receiver from the truncated bit stream. A description of the nonlinear multiresolution decomposition (with some derivatives) is given in section 2.

An application is presented in lossless image compression. Many of the existing lossless image codecs do not use a multiresolution decomposition hence they do not allow embedded coding. Moreover, they use either a fixed predictor filter (as in the S+P algorithm) or a context-based adaptive filter (as in CALIC codec [12]). In section 3 we give results of tests we have made after having implemented various derivatives of the above mentioned decomposition. We use either a non separable quincunx decimation or a separable decimation at a rate of two-to-one. FIR and ARMA reconstruction filters have been tested. The behaviours of the different methods are presented as a function of the parameters. The varying parameters are the orders of the optimal filter and the number of level in the decomposition. A comparison between the performances of the different methods and the S+P algorithm [10] is then given.

2 Adapted nonlinear decomposition

The general principle of the subband decompositions we have implemented is shown in the block diagram of Fig. 1, in the case of a one-level decomposition. The input image I is transformed into four subim-

ages. One of them, $I_{\ell\ell}$, results only from a decimation applied to I. It is the low resolution subimage. The others are the detail subimages. For a two-level decomposition, $I_{\ell\ell}$ is processed with the same algorithm and hence is transformed into four subimages. The same process is carried on for multilevel decompositions.
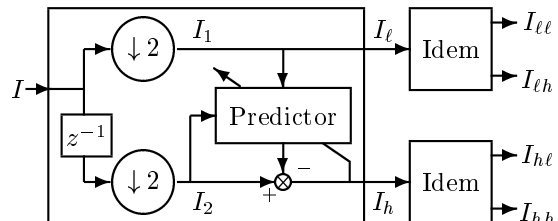
Figure 1: *One-level subband decomposition. The z^{-1} block corresponds to a one row (or column) shift in order to decompose I into the two sub-images I_1 and I_2 without loss of information.*

The image I is an array with M rows and N columns. Each pixel is coded with K bits. The image I is partitioned into two subimages I_1 and I_2 with a decimation at a rate of two-to-one. We have chosen two kinds of decimation: a quincunx one and a separable one. In the quincunx case, the image I is rotated of $\pi/4$ before the down-sampling, this gives two diamond-shape subimages which are completed with zeros in order to be represented by the matrices I_1 and I_2. In the separable case, the down-sampling is alternatively applied to the rows and to the columns. In the following, M_2 and N_2 denote respectively the numbers of rows and columns of I_2. After the decimation, the image I_2 is estimated according to the linear relation

$$\hat{I}_2(i,j) \;=\; \sum_{(h,k)\in\Delta_1} a_{hk} I_1(i-h, j-k) \\ + \sum_{(h,k)\in\Delta_2} b_{hk} I_2(i-h, j-k), \quad (1)$$

where Δ_1 and Δ_2 are finite subsets of rational integers (i.e. natural numbers and their opposites). We

have tested different domains Δ_1 and Δ_2 (see section 3). The coefficients a_{hk} and b_{hk} are computed in order to minimize the mean square error

$$W = \sum_{i=1}^{M_2} \sum_{j=1}^{N_2} \left(I_2(i,j) - \hat{I}_2(i,j) \right)^2. \qquad (2)$$

In the relations (1) and (2), the subimages I_1 and I_2 are completed by zeros. A first step of the one-level decomposition consists in the transformation of the image I into the two subimages I_ℓ and I_h given by the relations

$$I_\ell \;=\; I_1 \qquad (3)$$
$$I_h(i,j) \;=\; I_2(i,j) - \texttt{round}[\hat{I}_2(i,j)] \qquad (4)$$

(where $\texttt{round}[x]$ refers to the nearest integer of the real number x) for all the pixels (i,j) of I_2. The same algorithm (where the decimation on the rows is replaced by the decimation on the columns in the case of a separable down-sampling) is then applied to each of the two subimages I_ℓ and I_h in order to give the four subimages $I_{\ell\ell}$, $I_{\ell h}$, $I_{h\ell}$ and I_{hh}.

Let us introduce the z-transforms $I_2(z_1, z_2)$, $I_1(z_1, z_2)$ and $I_h(z_1, z_2)$ of respectively $I_2(i,j)$, $I_1(i,j)$ and $I_h(i,j)$ and the transfer functions

$$A(z_1, z_2) = \sum_{(h,k) \in \Delta_1} a_{hk} z_1^h z_2^k \qquad (5)$$

$$B(z_1, z_2) = \sum_{(h,k) \in \Delta_2} b_{hk} z_1^h z_2^k. \qquad (6)$$

If we neglect the nonlinearity (i.e. the function $\texttt{round}[\;]$ in the relation (4)) we obtain

$$\begin{aligned} I_h(z_1, z_2) &= -A(z_1, z_2) I_1(z_1, z_2) \\ &\quad + [1 - B(z_1, z_2)] I_2(z_1, z_2) \end{aligned} \qquad (7)$$

and hence

$$I_2(z_1, z_2) = \frac{I_h(z_1, z_2) + A(z_1, z_2) I_1(z_1, z_2)}{1 - B(z_1, z_2)}. \qquad (8)$$

In order to reconstruct the subimage I_2 from I_1 and I_h, the subset Δ_2 must be chosen in such a way that the filter $\frac{1}{1 - B(z_1, z_2)}$ is causal or semi-causal. Moreover, this filter can be unstable and therefore a test of

stability is required (see [2] for 2D recursive filter stability tests). When the coefficients b_{hk} are adapted to the input image, the filters stability must be tested for each input image and this takes a lot of CPU time. The problem of stability tests disappears by introducing the nonlinearity in the relation (4).

For image coding applications, the filter coefficients must be transmitted to the decoder. In order to simplify their transmission, we truncate the digits of their fractional part according to the relation

$$\hat{a}_{hk} = \texttt{round}[S * a_{hk}]/S \qquad (9)$$

(and a similar relation with b_{hk}), where the scale S is a natural number (in our tests $S = 10^6$). Let $\tilde{I}_2(i,j)$ be the left side of the relation (1), when the filter coefficients in the right side are replaced by $\hat{a}_{hk}$ and $\hat{b}_{hk}$. Therefore $\hat{I}_2$ must be replaced by $\tilde{I}_2$ in the relation (4) in order to permit perfect reconstruction of I_2 from I_ℓ and I_h:

$$I_2(i,j) = I_h(i,j) + \texttt{round}[\tilde{I}_2(i,j)]. \qquad (10)$$

Moreover, it is better to apply the decomposition to a zero mean image I, because under this condition the correlation between the pixel $I_h(i,j)$ and the pixels $I_\ell(i-h, j-k)$ in the neighborhood $(h,k) \in \Delta_1$ of $I_\ell(i,j)$ vanishes when we neglect the effects of the non linearity in the relation (4) and the difference between $\hat{I}_2$ and $\tilde{I}_2$. In order to perfectly reconstruct the image I from the four subimages $I_{\ell\ell}$, $I_{\ell h}$, $I_{h\ell}$ and I_{hh}, the transmission of a few parameters is required. These parameters are the dimension M, N of I, the filters orders, the filters coefficients $\hat{a}_{hk}$, $\hat{b}_{hk}$, the mean of I and the level L of decomposition. Indeed, it is easy to reverse the relations (3) and (4) when the region of support Δ_2 in the relation (1) is a non-symmetric half-plane or a quarter-plane.

We have also implemented nonlinear decompositions nearly identical to the above mentioned ones. The difference lies in the introduction of the S-transform [10] in the process, after the down-sampling and before the filtering. The subimages $I_1(i,j)$ and $I_2(i,j)$ are then respectively replaced, in the relations (1) and (2), by $I_1'(i,j)$ and $I_2'(i,j)$ so

that

$$I_1'(i,j) = \texttt{floor}[(I_1(i,j) + I_2(i,j))/2] \quad (11)$$

$$I_2'(i,j) = I_1(i,j) - I_2(i,j) \quad (12)$$

(where $\texttt{floor}[x]$ refers to the downward truncation of the real number x). The S-transform is applied at each stage, i.e. at the stage that decomposes the subimage I_ℓ into $I_{\ell\ell}$ and $I_{\ell h}$, at the stage that decomposes the subimage I_h into $I_{h\ell}$ and I_{hh}, and so on for a multi-level decomposition. Since the sum and the difference of two integers give either two odd or two even integers, the S-transform is reversible [10]:

$$I_1(i,j) = I_1'(i,j) + \texttt{floor}\left[\frac{I_2'(i,j) + 1}{2}\right] \quad (13)$$

$$I_2(i,j) = I_1(i,j) - I_2'(i,j). \quad (14)$$

3 Progressive lossless image coding

Let us introduce different acronyms in order to describe the algorithms we have implemented. Pyramidal RLMSE (Rounded Linear Mean Square Estimation) is the generic name of all the methods. The qualifier—either FIR or ARMA—specifies whether the filters in the relation (8) are either with a Finite Impulse Response (i.e. $B(z_1, z_2) = 0$,

$$\Delta_1 = \left\{(h,k) \in \mathbb{Z}^2 \mid |h| \le p \text{ and } |k| \le q\right\} \quad (15)$$

and Δ_2 is the empty set) or Auto-Regressive with Moving Average (i.e.

$$\Delta_2 = \left\{(h,k) \in \mathbb{Z}^2 \left| \begin{array}{ccc} 0 < h \le p & \text{and} & |k| \le q \\ & \text{or} & \\ 0 < k \le q & \text{and} & h = 0 \end{array} \right.\right\} \quad (16)$$

and Δ_1 is given in the relation (15)). The numbers p and q are the orders of the filter. We also specify the down-sampling type: either separable or quincunx. All the encoded images have the parameters $M = N = 512$ and $K = 8$. In table 1, we show the variations of the first order entropy of the transformed image with respect to both the orders (p,q) of the filter and the level L of decomposition for a

$(p,q)\backslash L$	2	3	4	5	6	
(1,1)	5.30	5.07	5.02	5.01	5.00	(a)
(1,2)	5.28	5.05	5.00	4.99	4.98	
(2,2)	5.27	5.03	4.98	4.97	4.97	

$(p,q)\backslash L$	2	3	4	5	6	
(1,1)	5.33	5.11	5.06	5.05	5.05	(b)
(1,2)	5.32	5.09	5.04	5.03	5.03	
(2,2)	5.30	5.07	5.02	5.01	5.01	

$(p,q)\backslash L$	2	3	4	5	6	
(1,1)	5.38	5.12	5.06	5.04	5.04	(c)
(1,2)	5.35	5.09	5.03	5.02	5.01	
(2,2)	5.34	5.07	5.01	5.00	5.00	

Table 1: First order entropy of the transformed image by the pyramidal RLMSE algorithm with a quincunx decimation and ARMA filters (a), FIR filters (b) or ARMA filters associated with the S-transform (c). The image is Goldhill 512.

pyramidal RLMSE algorithm with a quincunx decimation and either ARMA filters (a), or FIR filters (b), or ARMA filters associated with the S-transform (c). In table 2 (a), (b) and (c) the same variations with a separable decimation are shown. In table 3 we present the first order entropy of the image obtained with the S+P transform whose filter gives the smallest entropy (it is predictor B [10]). In table 4, 5 and 6 we show the variance (i.e. the ratio of the mean square error over the number of pixels) of the transformed image for the same algorithms as in table 1, 2 and 3 respectively. All the presented results have been obtained with the image Goldhill.

It is well known [10] that the minimum of the variance does not generally coincide with the minimum of the first order entropy, when parameters vary. Nevertheless, in our tests of pyramidal RLMSE algorithms these minima are generally close. It is not easy to compare various multiresolution decompositions in the aim of lossless image coding, because the discerning criteria in this case is the size of the bit stream after the reversible encoding of the transformed image. Therefore, the performances of the codec depend on the reversible encoder applied to the transformed

$(p,q)\backslash L$	2	3	4	5	6	
(1,1)	5.25	5.02	4.97	4.96	4.95	
(1,2)	5.24	5.01	4.95	4.94	4.94	(a)
(2,2)	5.23	5.00	4.95	4.93	4.93	
$(p,q)\backslash L$	2	3	4	5	6	
(1,1)	5.27	5.04	4.99	4.98	4.98	
(1,2)	5.27	5.04	4.99	4.98	4.98	(b)
(2,2)	5.26	5.04	4.98	4.97	4.97	
$(p,q)\backslash L$	2	3	4	5	6	
(1,1)	5.31	5.05	4.99	4.97	4.97	
(1,2)	5.30	5.04	4.97	4.95	4.95	(c)
(2,2)	5.29	5.03	4.96	4.95	4.95	

$(p,q)\backslash L$	2	3	4	5	
(1,1)	216.98	114.12	90.33	84.61	
(1,2)	215.08	112.10	88.17	82.33	(a)
(2,2)	212.55	109.33	85.34	79.59	
$(p,q)\backslash L$	2	3	4	5	
(1,1)	223.64	121.82	98.52	92.95	
(1,2)	221.52	119.56	96.16	90.57	(b)
(2,2)	219.92	117.76	94.26	88.67	
$(p,q)\backslash L$	2	3	4	5	
(1,1)	218.40	116.58	93.20	87.95	
(1,2)	213.70	111.27	87.66	82.35	(c)
(2,2)	211.24	108.47	84.71	79.39	

Table 2: First order entropy of the transformed image by the pyramidal RLMSE algorithm with a separable decimation and ARMA filters (a), FIR filters (b) or ARMA filters associated with the S-transform (c). The image is Goldhill 512.

Table 4: Variance of the transformed image by the same pyramidal algorithms as in table 1.

S+P$\backslash L$	2	3	4	5	6
S+P	5.21	5.01	4.96	4.95	4.95

Table 3: First order entropy of the S+P transform. The image is Goldhill 512.

image. However, the first order entropy of the transformed image gives an indication of the ability of the pyramidal RLMSE algorithms to lossless image coding. We have implemented an embedded zero-tree coding applied to the transformed image, following the SPIHT method described in [9]. In table 7, the compression bit rate obtained with the reversible encoding applied after pyramidal RLMSE decompositions is given and compared with the S+P transform, for different images.

4   Conclusion

We have presented an adapted nonlinear multiresolution decomposition (with some derivatives) of still images that permits perfect reconstruction. It is a hierarchical pyramidal decomposition with maximal decimation. The decomposition and reconstruction filterbanks are based on rounded linear mean square estimations. With ARMA reconstruction filters, the rounding applied to the output ensures the stability of the system, even when the ARMA filter is BIBO unstable.

An application in lossless image coding has been presented. Let us emphasize that the adapted multiresolution decomposition described in this paper allows embedded zero-tree coding. The performances of our decomposition and of the S+P transform have been compared. It appeared that our decomposition has a greater coding gain for IRM images.

References

[1] M. D. Adams and F. Kossentini, "Reversible Integer-to-Integer Wavelet Transforms for Image Compression: Performance Evaluation and Analysis", IEEE Transactions on Image Processing, vol. 9, no. 6, pp. 1010-1024, Jun. 2000.

[2] M. Barret and M. Benidir, "Behaviour of stability tests for two-dimensional digital recursive filters when faced with rounding error", IEEE Transactions on Circuits and Systems (II), vol. 44, no. 4, pp. 319–323, Apr. 1997.

$(p,q)\backslash L$	2	3	4	5	
(1,1)	209.59	106.45	82.41	76.73	(a)
(1,2)	208.81	105.56	81.43	75.67	
(2,2)	207.54	104.00	79.74	74.05	
$(p,q)\backslash L$	2	3	4	5	
(1,1)	217.96	115.57	91.95	86.46	(b)
(1,2)	217.88	115.45	91.77	86.25	
(2,2)	217.23	114.65	90.90	85.48	
$(p,q)\backslash L$	2	3	4	5	
(1,1)	209.10	105.88	81.8	76.37	(c)
(1,2)	207.82	104.54	80.44	74.99	
(2,2)	206.06	102.56	78.43	73.03	

Table 5: Variance of the transformed image by the same pyramidal algorithms as in table 2.

S+P$\backslash L$	2	3	4	5
S+P	209.51	106.34	82.50	77.09

Table 6: Variance of the transformed image by the S+P transform.

image	QD	QD+S	SD	SD+S	S+P
Lena	4.27	4.32	4.30	4.25	4.16
Goldhill	4.82	4.86	4.81	4.78	4.75
IRM 1	3.10	3.41	3.07	3.23	3.12
IRM 2	3.16	3.54	3.35	3.30	3.30
(a)					
image	QD	QD+S	SD	SD+S	S+P
Lena	4.27	4.33	4.29	4.25	4.16
Goldhill	4.83	4.85	4.82	4.79	4.75
IRM 1	3.16	3.41	3.14	3.21	3.12
IRM 2	3.26	3.54	3.00	3.30	3.30
(b)					

Table 7: Size of the bit stream in bit/pixel for pyramidal RLMSE+ARMA filters of order—either (1,2) in (a) or (2,1) in (b), $L = 5$, QD = quincunx decimation, SD = separable decimation, +S = with S-transform. For each image, the value in the S+P column is the smallest among the predictors A, B and C ([10]).

[3] Y.-S. Chung and M. Kanefsky, "On 2D recursive LMS algorithms using ARMA prediction for ADPCM encoding of Images", IEEE Transactions on Image Processing, vol. 1, no. 3, pp. 416–422, Jul. 1992.

[4] O. Egger, W. Li and M. Kunt, "High compression image coding using an adaptive morphological subband decomposition", Proceedings of the IEEE, vol. 83, no. 2, Feb. 1995.

[5] Ö. N. Gerek, A. E. Çetin, "Adaptive polyphase subband decomposition structures for image compression", IEEE Transactions on Image Processing, vol. 9, no. 10, pp. 1649–1660, Oct. 2000.

[6] F. J. Hampson and J. C. Pesquet, "M-band nonlinear subband decomposition with perfect decomposition", IEEE Transactions on Image Processing, vol. 7, no. 11, pp. 1547–1560, Nov. 1998.

[7] V. N. Ramaswamy, N. Ranganathan and K. R. Namuduri, "Performance analysis of wavelets in embedded zerotree-based lossless image coding schemes", IEEE Transactions on Signal Processing, vol. 47, no. 3, pp. 884–889, Mar. 1999.

[8] P. Roos, M. A. Viergever, M. C. A. Van Dijke and J. H. Peters, "Reversible intraframe compression of medical images", IEEE Transactions on Medical Imaging, vol. 7, no. 4, Dec. 1988.

[9] A. Said and W. A. Pearlman, "A new, fast and efficient image codec based on set partitioning in hierarchical trees", IEEE Transactions on Circuits and Systems for Video Technology, vol. 6, no. 3, pp. 243–250, Jun. 1996.

[10] A. Said and W. A. Pearlman, "An image multiresolution representation for lossless and lossy compression", IEEE Transactions on Image Processing, vol. 5, pp. 1303–1310, Sep. 1996.

[11] J. M. Shapiro, "Embedded image coding using zerotrees of wavelet coefficients", IEEE Transactions on Signal Processing, vol. 41, no. 12, pp. 3445–3462, Dec. 1993.

[12] X. Wu and N. Memon, "Context-based, Adaptive, Lossless Image Coding", IEEE Transactions on Communications, vol. 45, no. 4, pp. 437–444, Apr. 1997.